Gill Respiratory Morphometrics

Chapter · December 2011

DOI: 10.1016/B978-0-12-374553-8.00166-0

1 author:

Nicholas C. Wegner
National Marine Fisheries Service
60 PUBLICATIONS **1,317** CITATIONS

SEE PROFILE

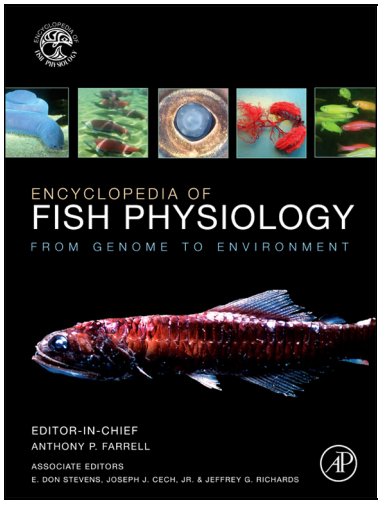

Wegner N.C. (2011) Gill Respiratory Morphometrics. In: Farrell A.P., (ed.), *Encyclopedia of Fish Physiology: From Genome to Environment*, volume 2, pp. 803–811. San Diego: Academic Press.

Gill Respiratory Morphometrics

NC Wegner, Scripps Institution of Oceanography, La Jolla, CA, USA

Glossary

Diffusion capacity Rate of gas transfer across a respiratory surface per unit of gas partial pressure (usually expressed in ml min^{-1} $mmHg^{-1}$). Dependent on the Krogh coefficient, the respiratory surface area, and the diffusion distance. Also often referred to as the gas transfer factor.

Gill arch Bony or cartilaginous support from which gill filaments extend into the branchial cavities.

Gill filaments (= primary lamellae) Elongated, blade-like structures that extend from the gill arch in the posterior–lateral direction.

Gill lamellae (i.e., secondary lamellae; sing. lamella) Thin folds or plates arising from the gill filaments that contain blood capillaries and serve as the site of gas exchange in the gills of most fishes (singular = lamella).

Gill resistance Resistance to water flow through the gills (= pressure head across the gills divided by the total volumetric flow of the ventilatory stream).

Gill respiratory morphometrics Dimensions of the gills that affect gas transfer between the water and blood.

Krogh coefficient Conductance of a solute (e.g., oxygen) through a particular respiratory medium (e.g., water and blood) or structure (e.g., the water–blood barrier).

Lamellar frequency Number of lamellae per unit length of filament (usually reported per mm). It is also referred to, in some texts, as lamellar density.

Total filament length Sum of the lengths of all filaments in the gills of a fish.

Total gill surface area Area of the gill respiratory epithelium in a fish; Normally reported as the bilateral surface area of all the gill lamellae.

Water–blood barrier thickness Thickness of the tissue barrier through which gases are exchanged between the interlamellar water and blood capillaries. This barrier consists of epithelial cells, a basement membrane, and the flanges of pillar cells. This is also referred to as water–blood barrier distance.

Abbreviations

$\dot{V}_{O_2}$	rate of oxygen uptake (ml O_2 min^{-1})
K	Krogh (= diffusion) coefficient (ml O_2 μm cm^{-2} $mmHg^{-1}$ min^{-1})
A	total gill surface area (cm^2)
ΔP_{O_2}	difference in the partial pressure of oxygen between blood and water at the gills (mmHg)
t	diffusion distance (μm)
D	diffusion capacity (ml O_2 min^{-1} $mmHg^{-1}$)
L_{fil}	total filament length (cm)
n_{lam}	lamellar frequency (number of lamellae per unit length of gill filament) (mm^{-1})
A_{lam}	mean bilateral surface area of an individual lamella (mm^2)
R	gill resistance (Pa s cm^{-3})
μ	dynamic viscosity of water (Pa s)
l	length of the interlamellar channels (= lamellar length) (μm)
d	diameter (= width) of interlamellar channels (μm)
w	width or thickness of a lamella (μm)
h	height of gill lamellae (μm)
b	species-specific scaling exponent, regression coefficient

Encyclopedia of Fish Physiology: From Genome to Environment, 2011, Vol. 2, 803-811, DOI: 10.1016/B978-0-1237-4553-8.00166-0

Introduction

Gills are the primary site of respiratory gas exchange in most fishes. Oxygen acquisition from the environment involves diffusion along a concentration gradient from the ventilatory water stream, across the gill epithelium, and into the blood. The rate of this process is described by the Fick equation:

$$\dot{V}_{O_2} = (K \times A \times \Delta P_{O_2})/t \quad (1)$$

where $\dot{V}_{O_2}$ is the rate of oxygen uptake, K is the diffusion or Krogh coefficient, A is the respiratory surface area of the gills, ΔP_{O_2} is the mean difference in the partial pressure of oxygen (=oxygen tension) between the blood and water, and t is the diffusion distance (see Abbreviations section for units associated with each term). This equation can be rearranged into the following form:

$$\dot{V}_{O_2}/\Delta P_{O_2} = (K \times A)/t = D \quad (2)$$

where the ratio of O_2 uptake to the mean difference in ΔP_{O_2} is referred to as the diffusion capacity (D). This term is independent of both the metabolic rate of the fish and the oxygen diffusion gradient across the gills and thus provides a useful metric to compare fish species in their ability to acquire environmental O_2 based on gill dimensions, where D depends on both the gill area and thickness of the respiratory epithelium (also called the water–blood barrier distance). This article discusses these morphometrics and their constituent parts (i.e., gill area can be subdivided into measures of the filaments and lamellae) in terms of methods for their measurement and theories on optimizing gas exchange, as well as the effects of fish habitat, metabolic demand, and growth on diffusion capacity.

Gill Morphology

Analysis of gill morphometrics with respect to gas exchange requires a basic understanding of fish branchial anatomy (for a comprehensive review of gill structure, the reader is directed to **Design and Physiology of Arteries and Veins**: Branchial Anatomy). Although varying in design and configuration, the gills of all jawed fishes have the same basic structural components: arches, filaments, and lamellae, which are illustrated for a typical teleost fish in Figure 1. Most fishes have four gill arches bilaterally positioned on each side of the oral cavity. Each arch supports two rows or sheets of gill filaments, long blade-like structures that extend away from the arch in the posterior-lateral direction (Figures 1(**a**) and 1(**b**)). Together, the two filament sheets constitute a holobranch; each individual row being called a hemibranch (i.e., half a holobranch). In teleosts, the hemibranchs of each arch are largely independent of each other and are connected only near their base by an interbranchial septum (Figure 1(**b**)). In elasmobranchs (sharks and rays), this septum extends from the gill arch out to the lateral edge of the fish (where it forms a gill flap), thereby binding the filaments of adjacent hemibranchs along their entire lengths (**see also Design and Physiology of Arteries and Veins**: Branchial Anatomy). In both configurations, the filaments of opposing hemibranchs from adjacent arches come together near their tips to form a continuous curtain or sieve through which the entire ventilatory stream passes (Figure 1(**b**)).

Each side of the filament blade supports a row of respiratory folds called lamellae (Figure 1(**c**)). Their plate-like morphology maximizes surface area while minimizing diffusion distances, thus allowing for effective and rapid gas exchange between blood and water. Blood, which flows in the opposite direction to the ventilatory water stream, is directed through the lamellae by the placement of pillar cells (Figure 1(**c**)) that extend across the blood lumen and connect the respiratory epithelium on either side (Figure 1(**d**)). The lamellar water–blood barrier is typically composed of two or more layers of epithelial cells, a basement membrane, and the flanges of pillar cells which form the inner lining of the lumen wall (Figure 1(**e**)). It may also contain mitochondria-rich cells (involved in osmoregulation and acid–base balance) and goblet cells (associated with mucus production) (**see also Role of the Gills**: Morphology of Branchial Ionocytes); however, in fishes with short diffusion distances, these specialized cells are often confined to the filament epithelium (as shown in Figure 1(**e**)).

Total Gill Surface Area

Total gill surface area refers to the area of the respiratory epithelium in a fish, which, in most species, is the bilateral surface of all the lamellae. Gill area (A) can thus be estimated using the equation:

$$A = L_{fil} \times 2n_{lam} \times A_{lam} \quad (3)$$

where L_{fil} is the total length of all the gill filaments, n_{lam} is the lamellar frequency (i.e., the mean number of lamellae per unit length on one side of a filament, which is multiplied by two to account for lamellae on each side), and A_{lam} is the mean bilateral surface area of a lamella. This classical method of estimating gill area takes advantage of the highly organized structure of the gills to methodically sample morphometrics at predetermined locations. With the exception of some flatfishes, the gills on either side of the head are symmetrical; thus, measurements for each dimension are generally only required from one side of the fish.

Total filament length is usually determined by counting all filaments from the gills on one side of the head,

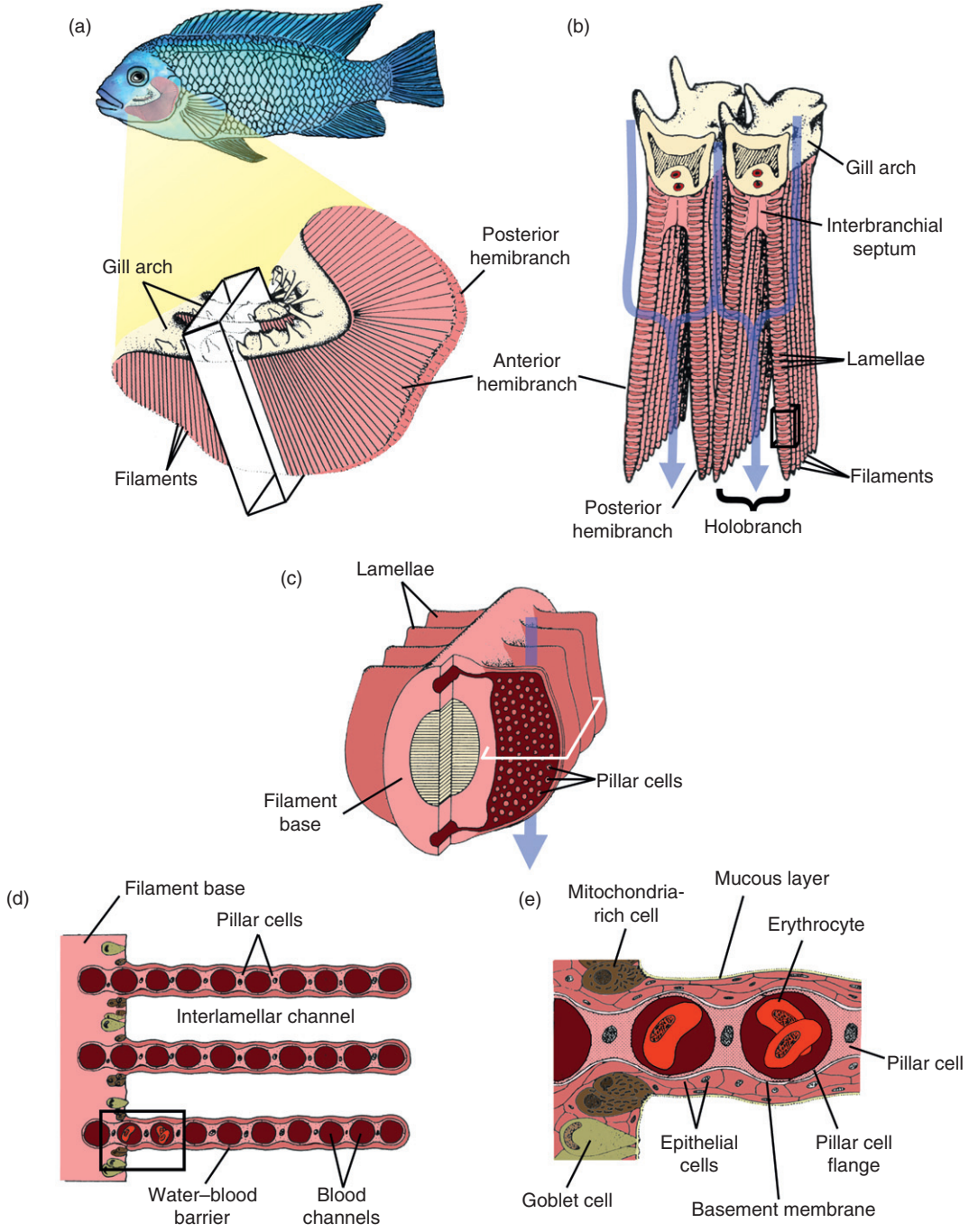

Figure 1 Gill morphology of a typical teleost: (a) anterior two gill arches from the left side of the head; (b) rotated and magnified section from (a) showing the placement and morphology of the two rows of gill filaments extending from each arch; (c) enlarged and rotated section from (b) showing the respiratory lamellae on both sides of a filament; (d) cross section through three adjacent lamellae from (c); (e) enlarged view from (d) showing the detail of the lamellar and filament epithelium. Water flow direction is indicated by blue arrows. Parts of this figure are modified or redrawn from Palzenberger M and Pohla H (1992) Gill surface area of water-breathing freshwater fish. *Reviews of Fish Biology and Fisheries* 2: 187–216.

and, depending on their abundance, dividing them into bins of 10, 20, or more on each arch (**Figure 2**(**a**)). The middle filament from each bin is measured and assumed to represent the mean filament length for that bin. The total length of all filaments in each bin can thus be calculated and these amounts are summed to estimate the total filament length for the gills on one side of the head. This amount is subsequently doubled to determine the total filament length for the entire fish. Lamellar frequency and bilateral surface area measurements are

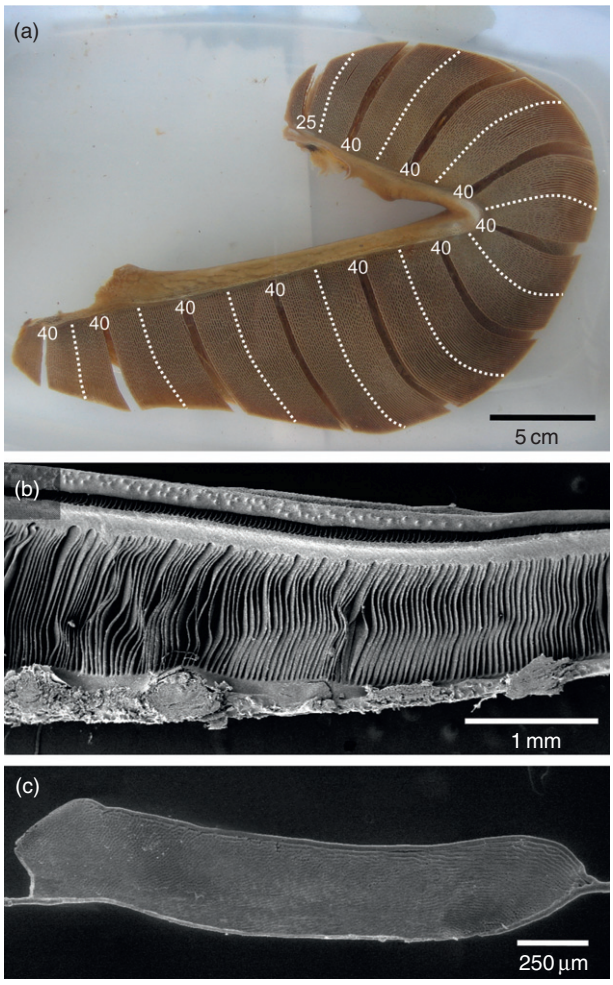

Figure 2 (a) Anterior hemibranch of the third gill arch from a 68-kg striped marlin, *Kajikia audax*, showing the division of 425 filaments into 10 bins of 40 and one bin of 25 (indicated by dotted white lines). The middle filament from each bin has been removed for measurements of lamellar frequency and bilateral surface area. (b) Scanning electron microscope (SEM) image of a selected gill filament used for determination of lamellar frequency. (c) SEM image of a corrosion-cast striped marlin lamella removed for determination of the bilateral surface area.

similarly made on each middle filament and assumed representative of their respective bins. Three measurements of each dimension are typically determined along the length of each filament to account for variation in lamellar shape, size, and spacing. For lamellar frequency, the filament is typically dissected from the arch (**Figure 2**(**a**)) and photographed under magnification near its base, middle, and tip (**Figure 2**(**b**)). Lamellae from these same locations are then dissected from the filament, mounted flat, and photographed to measure lamellar bilateral area (**Figure 2**(**c**)). Lamellar frequency and area measurements from each bin are weighted according to the filament length of that bin before being averaged (thus ensuring lamellar measurements from a bin with a longer filament length will contribute proportionately more toward the mean for the entire gills). Through extensive sampling of lamellar frequency and area on all four gill arches, one arch (usually the second or third) is typically found to be representative of the gills as a whole, and, thus, subsequent n_{lam} and A_{lam} measurements for that species can be made using only that arch.

More recently, gill surface area has also been estimated using stereological techniques. Randomly oriented gill tissue samples are embedded in glycol methacrylate or an alternative, and vertical sections through the tissue are mounted on slides and used to determine total gill volume. Subsequent point counting of filament and lamellar tissue densities using a superimposed grid allows calculation of their relative volumes and surface areas. This method is particularly useful in estimating the gill area of fishes that lack either highly organized and uniform filaments or two-dimensional lamellae. However, there have been few studies comparing the results obtained using stereological techniques with those of the more classic regional sampling method. In addition, stereological methods do not reveal the individual morphometrics contributing to gill area (i.e., L_{fil}, n_{lam}, and A_{lam}).

Diffusion Distances

Oxygen uptake at the gills requires diffusion through the interlamellar water, the water–blood barrier, and the blood plasma before passing through the red blood cell membrane and binding to hemoglobin. Although the widths of the interlamellar channels and lamellar blood vessels thus affect the length of the diffusion pathway, exact measurement of the total diffusion distance is confounded by convective processes of moving media (i.e., the diffusion distance depends on the thickness of boundary layers developing along the lamellar epithelium and other flow-related conditions). Thus, when referring to the diffusion capacity of the gills, emphasis is placed on the thickness of the water–blood barrier.

In most studies, this dimension is determined by viewing lamellar cross sections from multiple gill samples using light, scanning electron, or transmission electron microscopy and calculating the arithmetic mean thickness from measurements immediately overlaying lamellar blood channels (i.e., where the water–blood barrier is generally thin and most O_2 uptake likely occurs). Because diffusion also occurs through longer pathways overlying pillar cells, some studies calculate the harmonic mean thickness, in which averaging the reciprocals of measured lengths includes, but places less emphasis on, longer diffusion distances. In both methods, care must be taken to ensure that thickness measurements are made perpendicular to the plane of the gas-exchange surface, as oblique cross sections

result in longer measurements. In order to eliminate the potential for such errors, as well as sampling biases, application of stereological techniques developed for determining the air–blood barrier thickness in mammalian lungs probably provides the most accurate results. This involves vertical sectioning of randomly oriented gill tissue samples and calculates the harmonic mean thickness as $(2/3)l_h$, where l_h is the harmonic mean of all length measurements determined along parallel lines of a superimposed grid.

The use of varying techniques to measure barrier thickness can obscure interspecific comparisons (largely because arithmetic means tend to be shorter than harmonic means), and such complications can further be compounded in the calculation of gill diffusion capacity. A frequent error is coupling total gill area with the commonly reported arithmetic mean barrier thickness, which, because it only represents short diffusion distances overlaying blood vessels, causes an overestimation of diffusion capacity. More appropriate is pairing harmonic mean thickness with total gill area and the arithmetic mean with the surface area directly overlying blood channels, which, depending on the size and abundance of the pillar cells, is typically 20–40% lower than the total gill area. Other sources of error in determining gill morphometrics often result from poor tissue sample quality (i.e., gill tissue begins degradation within minutes of air exposure and requires immediate fixation upon collection).

Theories on Gill Dimensions

Despite various methods and difficulties associated with quantifying gill morphology, studies on a wide range of fish species have provided insight into the selective factors sculpting gill morphometrics. Of particular importance is the balance of having a sufficiently large gill area to meet metabolic demands while minimizing branchial resistance and thus the energetic costs of the cyclic buccal–branchial pumping mechanism used by most fishes to ventilate the gills. Because the interlamellar channels are the primary site of both oxygen uptake and gill resistance, this relationship can be examined through the Hagen–Poiseuille equation describing resistance (R) to water flow between parallel plates (i.e., through the lamellae). For a single interlamellar channel

$$R = 12\mu l/d^3 h \tag{4}$$

or for all interlamellar channels in the gills

$$R = 12\mu l(d + w)/d^3 h L_{\text{fil}} \tag{5}$$

where μ is the dynamic viscosity of the water, l is the interlamellar channel length, d is the diameter or width of the channel, w is the width or thickness of a lamella, and h is the lamellar height (dimensions shown in **Figure 3**). In fishes requiring a large gill area, an increase to lamellar length (l) or frequency (thus decreasing d) amplifies gill resistance and, consequently, the energy required to ventilate the gills. In contrast, an increase to lamellar height (h) or to the length of the gill filaments (L_{fil}) decreases gill resistance. Thus, from a purely energetic standpoint, gill area is optimally augmented through large (tall) lamellae and high total filament lengths.

Gill Morphometrics, Fish Habitat, and Metabolic Requirements

With the radiation of fishes into nearly every aquatic and semiaquatic niche, ranging from the open ocean to hypoxic swamps, both gill area and the water–blood barrier thickness can range more than an order of magnitude to meet specific demands associated with a species' physiochemical surroundings and metabolic requirements. As a result, distantly related taxonomic groups show remarkable evolutionary convergence for gill morphology, which has led to the categorization of fishes into different morphological ecotypes. Six major groups are recognized: (1) fast-swimming oceanic species, (2) marine fishes of intermediate activity, (3) sluggish marine species, (4) freshwater fishes,

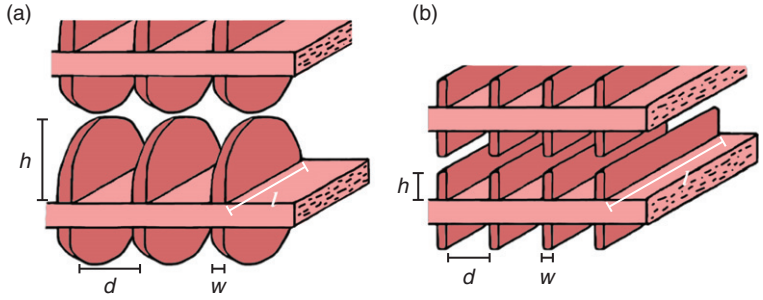

Figure 3 Typical arrangement and shape of the gill lamellae in (a) most teleosts and (b) most fast-swimming oceanic teleosts. *d*, interlamellar channel diameter (=~~width~~); *h*, lamellar height; *l*, lamellar length; *w*, lamellar thickness. Modified from Wegner NC, Sepulveda CA, Bull KB, and Graham JB (2010) Gill morphometrics in relation to gas transfer and ram ventilation in high-energy demand teleosts: Scombrids and billfishes. *Journal of Morphology* 271: 36–49.

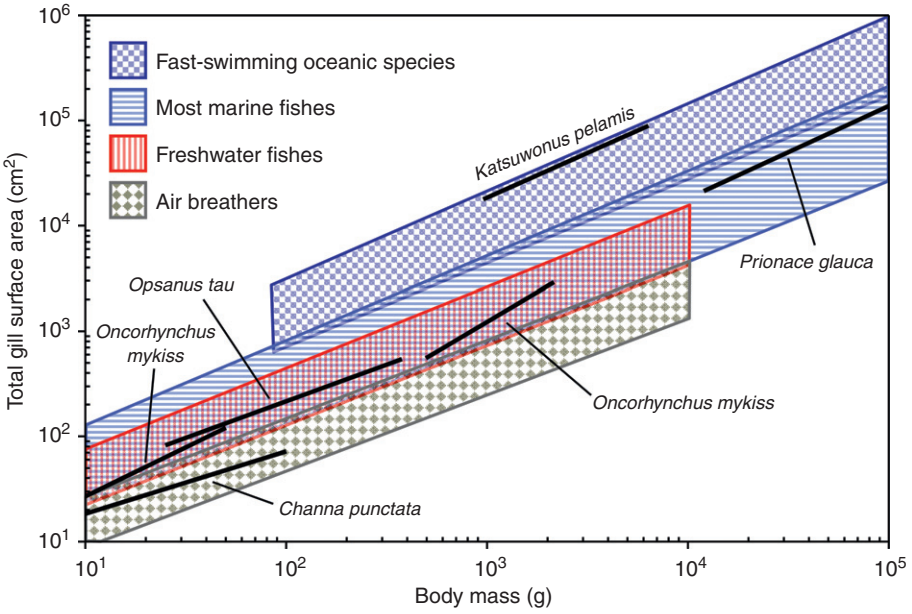

Figure 4 General relationships of gill surface area and body mass for different ecomorphological groups. For visual simplicity, marine fishes of intermediate activity and sluggish marine species are categorized together as most marine fishes. A regression line is shown for a representative of each group: (1) fast-swimming oceanic species, skipjack tuna, *K. pelamis*; (2) marine fish of intermediate activity, blue shark, *P. glauca*; (3) sluggish marine species, oyster toadfish, *O. tau*; (4) freshwater fish, rainbow trout, *O. mykiss*; and (5) air breather, spotted snakehead, *C. punctata*.

(5) air breathers, and (6) hypoxia dwellers. **Figure 4** compares the general range of gill surface area for each ecomorphological group with the exception of hypoxia dwellers, which includes fishes from groups 1–4 showing similar hypoxia-induced changes to gill morphology.

Fast-Swimming Oceanic Species

This group includes tunas and mackerels (family Scombridae), billfishes (Istiophoridae and Xiphiidae), dolphinfishes (Coryphaenidae), some jacks (Carangidae), and sharks of the family Lamnidae (e.g., the shortfin mako, *Isurus oxyrinchus*, and white shark, *Carcharodon carcharias*). These fishes generally have elevated energetic demands associated with fast, continuous swimming and high gill diffusion capacities resulting from large gill areas (which can be an order of magnitude greater than those of other marine fishes) and a thin water–blood barrier (approximately 0.5–1.2 μm). Both large gill areas and short diffusion distances reach their zenith in tunas, which accelerate metabolic processes through the retention of body heat produced by continuous swimming and have the highest O_2 demands of any fish group (**see also Pelagic Fishes**: Physiology of Tuna and Endothermy in Tunas, Billfishes, and Sharks). The largest relative gill area measured to date is that of the skipjack tuna, *Katsuwonus pelamis* (**Figure 4**).

For tunas and other fast-swimming oceanic teleosts, large gill areas generally result from numerous and long gill filaments with high lamellar frequencies (>30 mm^{-1} in some species). The increased number of filaments is achieved through changes to lamellar design, from a semicircular or triangular shape, typical of most fishes (**Figure 3**(**a**)), to a long, rectangular contour with a low profile (height) (**Figures 2**(**c**) and **3**(**b**)), thus allowing filaments to be closely spaced (**Figure 3**(**b**)). This shaping also allows for a marked reduction in the thickness of the water–blood barrier (i.e., low-profile lamellae require less structural support than tall lamellae) contributing to generally thin lamellae (only 5–6 μm in scombrids and billfishes). This reduced lamellar thickness, in conjunction with a narrow spacing between lamellae, increases lamellar frequency, which, in addition to augmenting gill area, decreases diffusion distances and minimizes physiological dead space in the interlamellar channels.

These changes to gill morphology deviate from the theoretical predictions for optimally augmenting gill area; the high frequency and unique shape of the lamellae narrow and lengthen the interlamellar channels (**Figure 3**(**b**)), which, according to Equations (4) and (5), increase gill resistance. Although a high branchial resistance substantially raises the energetic costs of gill ventilation in most fishes, it appears of less concern to fast oceanic species that breathe through ram ventilation, in which branchial flow is driven by fast, forward swimming rather than the pumping of the buccal and branchial cavities. In these fishes, the high branchial resistance associated with this unique morphometric configuration augmenting gill area helps to slow and streamline a fast and turbulent ram-ventilatory stream to

create favorable flow conditions for gas exchange in the interlamellar channels.

In contrast, the large gill areas of lamnid sharks are achieved in the predicted manner: long gill filaments with relatively large lamellae. This likely reflects flow constraints imposed by the elasmobranch gill design in which water passing between the gill lamellae must subsequently flow through specialized channels along the interbranchial septum to exit the gill slits (**see also Design and Physiology of Arteries and Veins**: Branchial Anatomy). This additional water-flow pathway increases resistance through the elasmobranch gill and appears to preclude the recruitment of a high lamellar frequency to augment gill area (which would further augment branchial resistance). The relatively large lamellae of lamnid sharks appear to require additional structural support through a slightly thicker water–blood barrier (~1.2 μm in the shortfin mako, in comparison to 0.5 μm in tunas).

Marine Fishes of Intermediate Activity

This is largely a heterogeneous group of fishes characterized mainly by gill areas that are smaller than those of highly active oceanic species and larger than those of sluggish fishes. Included in this group are most marine fishes studied to date, including many jack species, mullets (Mugilidae), porgies (Sparidae), seabasses (Serranidae), wrasses (Labridae), butterfishes (Stromateidae), croakers (Sciaenidae), puffers (Tetraodontidae), and sharks from the families Sphyrnidae and Carcharhinidae, including oceanic species such as the blue shark, *Prionace glauca* (Figure 4). Often referred to as Gray's intermediates (after IE Gray who conducted the first comprehensive comparative study of gill surface areas in the 1950s), the gills of these fishes are largely normal; the gill filaments are of average length and number, and although many of these species are capable of ram ventilation at faster swimming speeds, the lamellae are generally taller and more traditionally shaped than those of the more highly active species. In teleosts, lamellar frequencies typically range from 15 to 25 mm^{-1}, while in elasmobranchs, frequencies of 10–15 mm^{-1} are more common, likely reflecting flow constraints imposed by the interbranchial septum. The thickness of the water–blood barrier usually ranges from 1.5 to 6 μm.

Sluggish Marine Species

This group includes relatively inactive species usually associated with the benthos or ocean depths that have small gill areas. Fishes from the deep ocean such as the bristlemouths (Gonostomatidae), barbeled dragonfishes (Stomiidae), deepsea tripod fishes (Ipnopidae), and some cusk eels (Ophidiidae) typically have low total filament lengths resulting from generally short and widely spaced filaments. Lamellar frequencies are also reduced, ranging from 7 to 20 mm^{-1}, which minimizes branchial resistance and the energetic requirements of gill ventilation. In some groups, a direct correlation has been found between ocean depth and gill size, in which the smaller gills of deeper-dwelling species likely reflect reduced metabolic demands. In shallower waters, benthic species including flatfishes (Bothidae and Pleuronectidae), some elasmobranchs (Squalidae, Scyliorhinidae, Triakidae, Rajidae, and Torpedinidae), and toadfishes (Batrachoididae) also have reduced gill areas and, in some cases, the water–blood barrier can be quite thick (e.g., the small-spotted catshark, *Scyliorhinus canicula*, >11 μm), although this is not necessarily a distinguishing characteristic (e.g., the common sole, *Solea solea*, <3 μm). The well-studied oyster toadfish, *Opsanus tau*, has fairly large lamellae, but a small total filament length (resulting largely from only three gill arches on each side of the head) and low lamellar frequency (10–13 mm^{-1}) leading to a small gill area (Figure 4), which, when coupled with a relatively thick lamellar water–blood barrier (5–6 μm), results in a gill diffusion capacity 100× less than that of a comparably sized tuna.

Freshwater Fishes

The gill surface areas of these fishes are generally smaller than similar species inhabiting the marine environment. For example, the relatively active rainbow trout, *Oncorhynchus mykiss*, has a gill surface area similar to that of *O. tau* (Figure 4). This likely reflects several factors, including the reduced osmotic costs associated with life in freshwater and differences in dissolved oxygen levels (i.e., for a given temperature, air-saturated freshwater contains 15–20% more O_2). Despite an increase in O_2 availability, freshwater systems lack high-energy demand fishes comparable to those of the open ocean, which results in a reduced range in gill surface area. The largest gill areas of freshwater fishes thus approach those of marine species of intermediate activity (Figure 4) and are often associated with life in hypoxia (see below) or diadromy (the ability to inhabit both marine and freshwater environments). The smaller gill surface areas of freshwater fishes generally result from fairly small lamellae. The water–blood barrier thickness in freshwater fishes typically ranges from 2 to 10 μm which is similar to the combined range of intermediate and sluggish marine species.

Air Breathers

In order to exploit hypoxic habitats (**see also Hypoxia**: The Expanding Hypoxic Environment), many fishes have auxiliary air-breathing organs ranging from respiratory epithelia lining the mouth and digestive tract to gas bladders and lungs (**see also Air-Breathing Fishes**: The Biology, Diversity, and Natural History of Air-Breathing Fishes: An Introduction and Respiratory Adaptations for

Air-Breathing Fishes). Air offers the distinct advantage of containing much more O_2 per unit volume than water and being a less viscous respiratory medium, thus reducing ventilatory costs. The evolution of air breathing is often associated with a reduction in gill area (**Figure 4**), which minimizes the loss of oxygen acquired through an air-breathing organ to hypoxic water (**see also Air-Breathing Fishes**: Respiratory Adaptations for Air-Breathing Fishes). In many species, such as the lungfishes of the genera *Lepidosiren* and *Protopterus*, the gills have become so reduced that drowning occurs if air access is denied. However, most air-breathing fishes are facultative air breathers, meaning the gills are large enough to sustain aerobic metabolism in normoxia and air breathing is used primarily to supplement aquatic respiration under hypoxic conditions or during heightened O_2 demands associated with exercise. The water–blood barrier in air-breathing fishes is often quite thick, especially in amphibious species such as the climbing perch, *Anabus testudineus*, where it can exceed 10 μm and may help to limit gill desiccation and maintain lamellar structural integrity out of water. In nonamphibious air breathers, a thick water–blood barrier may work in conjunction with a small gill area to reduce oxygen loss to the hypoxic environment via the gills. However, many air-breathing fishes maintain relatively thin barriers (i.e, the spotted snakehead, *Channa punctata*, 2.0 μm) indicating the continued importance of the gills in aquatic respiration.

Hypoxia Dwellers

Fishes living in periodic or chronic hypoxia and lacking the ability to breathe air generally show changes to gill morphology that increase diffusion capacity. Specifically, inhabitants of hypoxic swamps, including some African cichlids (Cichlidae), elephantfishes (Mormyridae), cyprinids (Cyprinidae), livebearers (Poeciliidae), characids (Characidae), and trahiras (Erythrinidae), as well as fishes living in the ocean's oxygen minimum zone (OMZ), such as bristlemouths, pearleyes (Scopelarchidae), and bigscale fishes (Melamphaidae) or hypoxic tidepools, including sculpins (Cottidae), usually have larger gill areas than conspecifics or closely related species living in normoxic waters. Unlike high-energy demand teleosts, gill areas in hypoxia dwellers are generally augmented through relatively large lamellae and long gill filaments, thus maintaining low energetic costs for gill ventilation. Few measures of the water–blood barrier thickness exist for such fishes, although it is hypothesized that they should be fairly thin.

Hypoxia-induced changes to gill morphometrics depend on both the severity and periodicity of low O_2 levels. On evolutionary timescales, selective pressures for the exploitation of nutrient-rich waters in the OMZ have resulted in a number of mesopelagic species specialized for life in chronic hypoxia, such as the pearl eye, *Scopelarchoides nicholsi*, which has such long gill filaments they protrude from the opercular openings (**Figure 5**). In environments with prolonged but periodic hypoxia (e.g., many freshwater swamps), phenotypic plasticity in gill morphology allows for adjustment to changing conditions on shorter timescales. For example, African cichlids reared in the laboratory under hypoxic conditions have longer filaments and higher gill surface areas than those raised in normoxia. Such plasticity in gill morphology is epitomized by the crucian carp, *Carassius carassius*, which, when exposed to hypoxia in ice-covered ponds during the winter, can increase gill area by 7.5× ~~in~~ 7–14 days by exposing lamellae normally embedded in an interlamellar cellular mass (**see also Ventilation and Animal Respiration**: Plasticity in Gill Morphology).

Scaling: Fish Gill Morphometrics in Relation to Fish Growth

Gill surface area and its componential dimensions are often reported in relation to fish body mass using log–log plots (**Figure 4**) and the power-law scaling equation:

$$Y = aM^b \tag{6}$$

or log form

$$\log\ Y = \log\ a + b\ \log\ M \tag{7}$$

where Y is the particular gill morphometric (i.e., A, L_{fil}, n_{lam}, or A_{lam}), a is the intercept value for a 1-g specimen, M is the fish mass, and b is the species-specific slope or scaling exponent (=regression coefficient). As a fish grows, isometric geometry of the gills (i.e., the length/area/volume relationship assuming gill mass increases at the same rate as body mass, $b = 1.0$) predicts that L_{fil} should scale to the one-third (i.e., length/volume, $b = 0.33$), n_{lam} to the negative one-third (length^{-1}/volume, $b = -0.33$), and A_{lam} to the two-thirds (area/volume, $b = 0.67$), which, when added together, sum to the expected scaling exponent for total gill

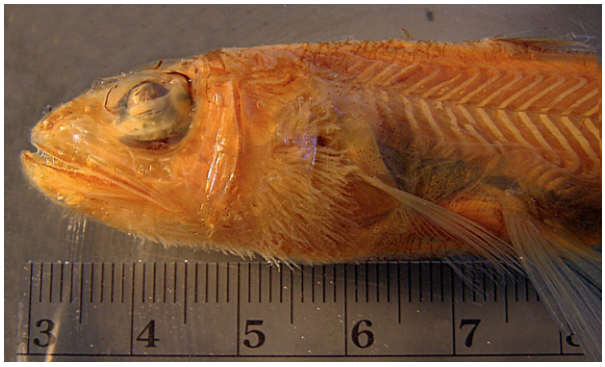

Figure 5 Elongate gill filaments of the pearleye, *Scopelarchoides nicholsi*, extending out the opercular slits. Scale is in cm.

surface area (area/volume, $b = 0.67$). However, in general, measured values do not conform to these geometric predictions, indicating the influence of various physiological processes affecting gill growth. For example, the scaling exponent for gill area ranges from under 0.50 to over 1.00. The mean of this range (0.80) appears to correlate with the mean scaling exponent for fish standard metabolic rate with body mass (0.81), while deviation from the mean may reflect a connection to active metabolic demands (e.g., in continuously swimming fishes which are never at rest) or other variables (**see also Energetics**: Physiological Functions that Scale to Body Mass in Fish). The low scaling exponents of many air-breathing fishes (e.g., *C. punctata*, $b = 0.59$; **Figure 4**) reflect an increased reliance on auxiliary air breathing with growth. At the opposite extreme, the hemoglobin-lacking blackfin icefish, *Chaenocephalus aceratus*, has a scaling exponent of 1.09, which appears to be associated with the increasingly problematic effects of diffusion limitation at larger body sizes.

By incorporating species-specific changes with mass, scaling equations facilitate interspecific comparisons of gill morphometrics and are often extrapolated to compare species of different body size. This has largely replaced methods of early gill studies comparing fishes of different weights through mass-specific gill areas (i.e., gill area/fish mass), which are generally inappropriate because gill area and body mass do not scale isometrically. Although the extrapolation of scaling equations thus provides a more favorable means of comparison, statistically, morphometric relationships can only be compared over a shared (i.e., overlapping) weight range. Errors associated with extrapolating gill area, or other morphometric relationships (especially those established using a limited sample size or weight range), can be seen in **Figure 4** where two independently determined regression lines for *O. mykiss* result in very different scaling equations.

See also: **Air-Breathing Fishes**: Circulatory Adaptations for Air-Breathing Fishes; Respiratory Adaptations for Air-Breathing Fishes; The Biology, Diversity, and Natural History of Air-Breathing Fishes: An Introduction. **Design and Physiology of Arteries and Veins**: Branchial Anatomy. **Energetics**: Physiological Functions that Scale to Body Mass in Fish. **Gas Exchange**: Respiration: An Introduction. **Hypoxia**: The Expanding Hypoxic Environment. **Pelagic Fishes**: Endothermy in Tunas, Billfishes, and Sharks; Physiology of Tuna. **Role of the Gills**: Morphology of Branchial Ionocytes; The Osmorespiratory Compromise. **Transport and Exchange of Respiratory Gases in the Blood**: O_2 Uptake and Transport: The Optimal P50. **Ventilation and Animal Respiration**: Efficiency of Gas Exchange Organs; Plasticity in Gill Morphology.

Further Reading

Chapman LJ (2007) Morpho-physiological divergence across aquatic oxygen gradients in fishes. In: Fernandes MN, Rantin FT, Glass ML, and Kapoor BG (eds.) *Fish Respiration and Environment*, pp. 13–39. Enfield, NH: Science Publishers.

Da Costa OTF, Predretti ACE, Schmitz A, Perry SF, and Fernandes MN (2007) Stereological estimation of surface area and barrier thickness of fish gills in vertical sections. *Journal of Microscopy* 225: 1–9.

Graham JB (1997) *Air-Breathing Fishes: Evolution, Diversity, and Adaptations*. San Diego, CA: Academic Press.

Graham JB (2006) Aquatic and aerial respiration. In: Evans DH and Claiborne JB (eds.) *The Physiology of Fishes*, 3rd edn., pp. 85–117. Boca Raton, FL: CRC Press.

Gray IE (1954) Comparative study of the gill area of marine fishes. *Biological Bulletin* 107: 219–225.

Hughes GM (1966) The dimensions of fish gills in relation to their function. *Journal of Experimental Biology* 45: 177–195.

Hughes GM (1970) Morphological measurements on the gills of fishes in relation to their respiratory function. *Folia Morphologica* 18: 78–95.

Hughes GM (1972) Morphometrics of fish gills. *Respiration Physiology* 14: 1–25.

Hughes GM (1980) Morphometry of fish gas exchange organs in relation to their respiratory function. In: Ali MA (ed.) *Environmental Physiology of Fishes*, pp. 33–56. New York: Plenum.

Hughes GM (1984) General anatomy of the gills. In: Hoar WS and Randall DJ (eds.) *Fish Physiology*, vol. 10A, pp. 1–72. Orlando, FL: Academic Press.

Hughes GM (1984) Measurement of gill area in fishes: Practices and problems. *Journal of the Marine Biological Association of the United Kingdom* 64: 637–655.

Hughes GM and Morgan M (1973) The structure of fish gills in relation to their respiratory function. *Biological Reviews of the Cambridge Philosophical Society* 48: 419–475.

Muir BS and Hughes GM (1969) Gill dimensions for three species of tunny. *Journal of Experimental Biology* 51: 271–285.

Palzenberger M and Pohla H (1992) Gill surface area of water-breathing freshwater fish. *Reviews in Fish Biology and Fisheries* 2: 187–216.

Stevens ED (1992) Oxygen molecules as units to dimension the sieve of fish gills. *Environmental Biology of Fishes* 33: 317–318.

Wegner NC and Graham JB (2010) George Hughes and the history of fish ventilation: From Du Verney to the present. *Comparative Biochemistry and Physiology – Part A: Molecular and Integrative Physiology* 157: 1–6.

Wegner NC, Sepulveda CA, Bull KB, and Graham JB (2010) Gill morphometrics in relation to gas transfer and ram ventilation in high-energy demand teleosts: Scombrids and billfishes. *Journal of Morphology* 271: 36–49.

Weibel ER and Knight BW (1964) A morphometric study on the thickness of the pulmonary air–blood barrier. *Journal of Cell Biology* 21: 367–384.